ULTRASONIC CHARACTERIZATION OF FATIGUE BEHAVIOR IN METAL-MATRIX COMPOSITES

R. Nuñez, J. Wahnschaffe, K. Salama
Mechanical Engineering Department
University of Houston
Houston, TX 77204-4792

INTRODUCTION

In the past decades, the incorporation of ceramic reinforcement in metal-matrix composites (MMC's) brought about considerable improvements in elastic modulus, strength, wear resistance, structural efficiency, reliability and control of physical properties (e.g. density and coefficient of thermal expansion) thereby providing for improved mechanical performance in comparison to the unreinforced matrix [1-4]. S-N curves for materials such as steels are available elsewhere [5-6] whereas are limited for MMC's. Studies on the elastic constants behavior for MMC's as a function of temperature, volume fractions of reinforcement and applied stresses had already been conducted [7-8]. However, the fatigue behavior of elastic constants in MMC's is not well understood. Further, the trend now is aimed at nondestructive evaluation (NDE) of materials which in the past years gained significant attention over the conventional destructive tests since the former is capable of determining the usefulness, serviceability or quality of a part or material without limiting its usefulness, which is not possible in the latter's case [9-10]. In view of the above discussion, a result of the study on the fatigue behavior and ultrasonic characterization of monolithic aluminum and aluminum MMC's will be discussed here.

EXPERIMENTAL

Material

Two materials selected for investigation in this study were based on an unreinforced Al 6092 alloy and its composite counterpart reinforced with 17.5 vol% SiC particulates. The actual chemical composition (in weight percent) of the unreinforced alloy (which is also the matrix of the composite) is given in Table 1. All materials were extruded and received in the form of sheets which were provided by DWA Composite Specialities, Inc. (Chatsworth, CA).

Review of Progress in Quantitative Nondestructive Evaluation, Vol. 16
Edited by D.O. Thompson and D.E. Chimenti, Plenum Press, New York, 1997

Table 1. Actual chemical composition (weight percent) of Al 6092 [11-12]

Element	Si	Fe	Cu	Mn	Mg	Cr	Zn	Ti	Zr	Others	Al
(%)	0.4-0.8	0.3	0.7-1.0	0.15	0.8-1.2	0.15	0.25	0.15	--	0.15	rem

Specimen description and preparation

Similar test specimen preparation techniques were used for both composite and unreinforced alloy. Rectangular blanks of length 16.5 cm were cut from the as-received materials using a diamond coated saw blade. Using a carbide-tipped cutting tool, the test specimens were precision machined from the rectangular blanks with the stress axis parallel to the extrusion direction as in [4,12]. These were smooth and rectangular in cross-section (1.27 cm x 2.54 cm) having a sufficient thickness for proper detection of backwall echoes. The specimen dimensions conform with ASTM Standard E 466, the standard procedure in conducting axial fatigue tests which recommends several different specimen shapes [13]. The length-to-width ratio was chosen so as to ensure that the test specimens would not buckle during load-controlled cyclic fatiguing. To minimize the effects of surface irregularities and finish, the specimens were hand polished as in [4] using silicon carbide impregnated emery paper of grit sizes 180, 320, 600 and 1,200. In addition, a special three-stage polishing method [9] was adapted in this experiment specifically patterned to polish the MMC's (i.e. to overcome the problems associated with the simultaneous polishing of a soft material like aluminum alloy and a hard material such as SiC_p reinforcement).

Fatigue Testing

Fatigue tests were performed on a closed-loop, servohydraulic materials testing system (MTS) equipped with a 9,072-kg load cell. Both low- and high-cycle axial fatigue tests were performed over a range of stress stress levels at a constant load ratio R of 0.1 and a frequency of 5 Hz following a sinusoidal waveform under load-controlled mode. The cyclic fatiguing was done in tension-tension to avoid buckling. The test machine was set and maintained at a constant cyclic stress, which is the controlled variable. The number of cycles to failure or separation was taken as the materials' fatigue life, N_f.

Introduction of opposite single U-shaped notches of 1.6-mm radius for each type of material was made. Similarly, opposite single U-shaped notches of 26-cm radius were also introduced in other specimens so as to compare the effects of each in the elastic constants behavior during fatigue cycling. This study made use of the average stress (AS) model [14-16] in the calculation of the fatigue notch factor K_f, which was used in fatigue tests calculations. The relationship between K_f and K_t, theoritical concentration factor generally used in monotonic tests can be found elsewhere [15-16]. The introduction of the aforementioned notches was done in order to create a localized stressed zone in the center of the specimen such that failure is expected to occur within or close to that region [12]. The formula used in fatigue calculation in this study is given by [15-16]:

$$\sigma_{peak} = \left(\frac{P_{peak}}{A_{ts}} \right) \cdot K_f \qquad (1)$$

where σ_{peak} is the peak stress (maximum stress); P_{peak} is the peak load; A_{ts} is the test section cross sectional area; and K_f is the fatigue notch factor.

Ultrasonic Non-Destructive Testing

In this study, ultrasonic pulse-echo overlap method [17] was used to obtain the *time-of-flight* (TOF). Videoscan Ultrasonic transducers 0.635 cm in diameter supplied by Panametrics [18] were used in this experiment, which both served as the transmitter and receiver. A micrometer with an accuracy of $\pm$ 5 μm was used to measure the thickness of all test specimens. Special couplants, each for longitudinal wave and shear wave *time-of-flight* measurements were used. Prior to fatiguing each test specimen, TOF measurements were conducted in several locations in the test specimens (see Figure 1) from which the calculations of ultrasonic velocities and elastic constants were based During fatigue cycling, interruptions at designated number of cycles for each particular stress level were done and the *time-of-flight* measurements at same positions were made. In addition, post-fracture ultrasonic measurements were also done. In this particular work, isotropy-based calculation of materials' elastic constants was adapted.

The materials' elastic constants were determined using the following equations:

$$\text{Longitudinal Modulus} = \rho \cdot v_l^2 \tag{2}$$

$$\text{Shear Modulus} = \rho \cdot v_s^2 \tag{3}$$

where ρ is the material density; v_l and v_s are the longitudinal and shear wave velocities, respectively. The values of the elastic constants reported here are the average values of the measurements obtained in two transducer positions closer to the middle part of the test specimens in Figure 1.

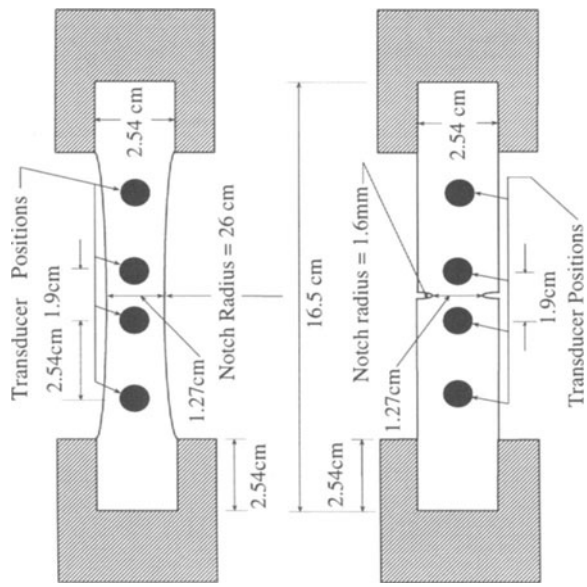

Figure 1. Schematic of specimen configuration for the fatigue test and ultrasonic velocity measurements. All dimensions in cm.

RESULTS AND DISCUSSION

Figure 2 shows the Peak Stress-Cycles to Failure plot for the monolithic aluminum and the composite at notch radius = 26 cm. At similar peak stress levels, the composite has a higher fatigue life than the monolithic aluminum. This means that for the composite, a higher peak stress than that of monolithic aluminum is needed for the former to fail and have same fatigue life as the latter. It is believed that the increase in strength in composite is due to the strengthening effect of the reinforcements present in its matrix [1-4].

The S-N plot for specimens at small notch radius = 1.6 mm. in Figure 3 shows a similar behavior to those specimens at large notch radius = 26 cm in Figure 2 except that a shift in the peak stress values for specimens at large notch over those at small notch is observed. This difference is thought to be associated with the sensitivity of K_f to K_t in the model used in this study [14-15]. It must be pointed out however, that the two plots in Figures 2 and 3 were mainly intended for the purpose of comparing the fatigue lives of the specimens under several peak stress levels. The accuracy of the N_f's reported here can be improved by performing additional tests under same conditions.

A plot showing the relationship between the longitudinal modulus as a function of the materials' fatigue life for the monolithic aluminum is shown in Figure 4. For specimens at large notch, a considerable increase in longitudinal modulus of up to 20% is observed. At lower fatigue lives of up to 5 x 10^4 cycles, an abrupt change in the modulus is evident. However, there are not much significant changes in longitudinal modulus

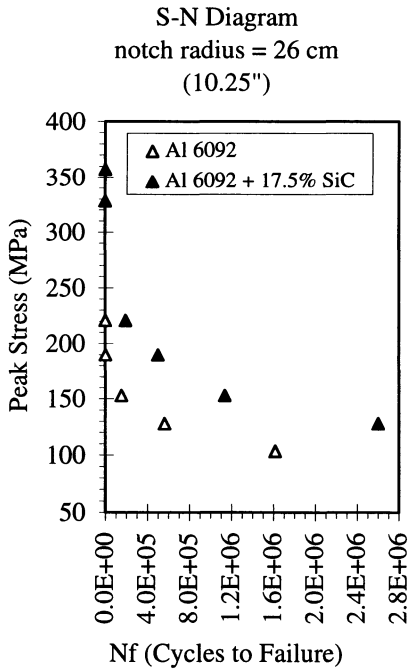

Figure 2. Peak stress-Cycles to Failure plot for specimens at notch radius = 26 cm.

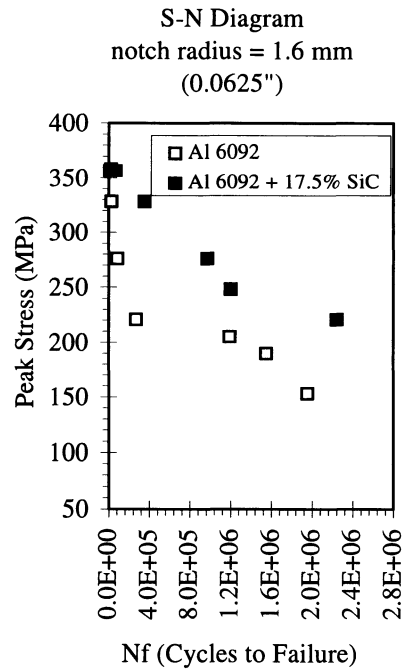

Figure 3. Peak Stress-Cycles to Failure plot for specimens at notch radius = 1.6 mm.

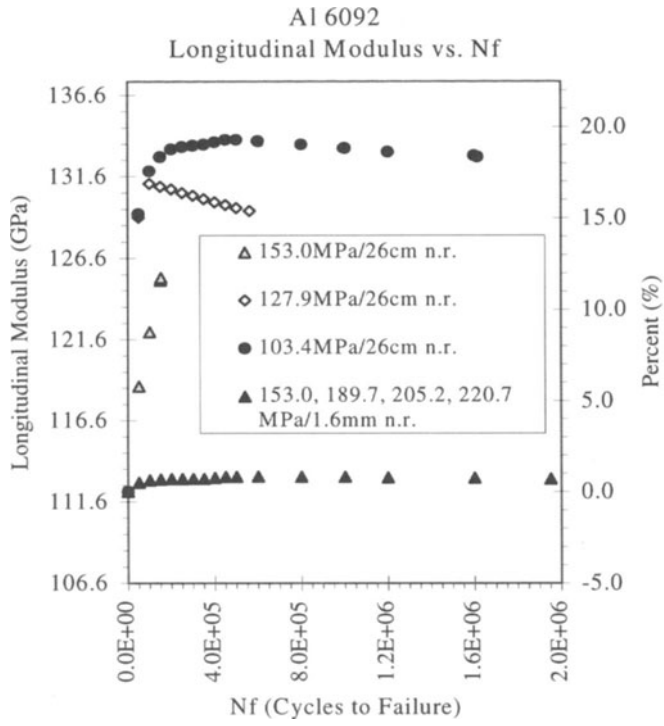

Figure 4. Longitudinal Modulus -Cycles to Failure plot for monolithic aluminum 6092 alloy.

behavior at higher fatigue lives. This behavior can be attributed to larger deformation (elongation) in the early fatigue lives (i.e. up to 5 x 10^4 cycles). At higher fatigue lives however, strain hardening is thought to have occured thereby no further significant increase in the longitudinal modulus is observed. The larger elongation found in large notched-monolithic specimens showed confirmation to such increase in longitudinal modulus at lower fatigue lives of 5 x 10^4 cycles and to smaller (or even undetectable) increase in longitudinal modulus at higher fatigue lives. However, for specimens at smaller notch, there is no significant increase in the longitudinal modulus. This behavior can be related to the K_f-K_t relationship as discussed above.

Figure 5 is a Longitudinal Modulus-Cycles to Failure plot for the Al 6092 + 17% SiC composite specimens subjected to fatigue cycling. An increase of up to only 2.5% in the longitudinal modulus is seen. This small increase in longitudinal modulus is expected as a consequence of the strengthening effect of SiC reinforcements in the monolithic aluminum matrix. Further, by comparing the increase in longitudinal modulus between the monolithic aluminum and the composite, a ratio of about 8 (i.e. 20/2.5) in the elastic moduli is obtained.

The Shear Modulus-Cycles to Failure plot in Figure 6 shows that for the monolithic aluminum at large notch = 26 cm., the shear modulus increases with decreasing stress, a similar behavior observed in the longitudinal modulus behavior in the same material at same notch in Figure 4. For the monolithic aluminum at small notch = 1.6 mm., there is not a significant increase in the shear modulus at all levels of its fatigue life.

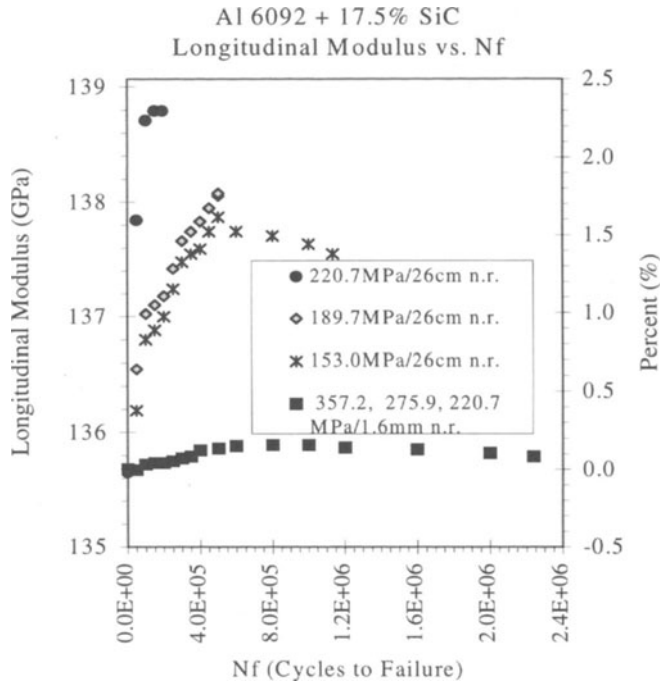

Figure 5. Longitudinal Modulus-Cycles to Failure plot for Al 6092 + 17.5% SiC_p composite specimens.

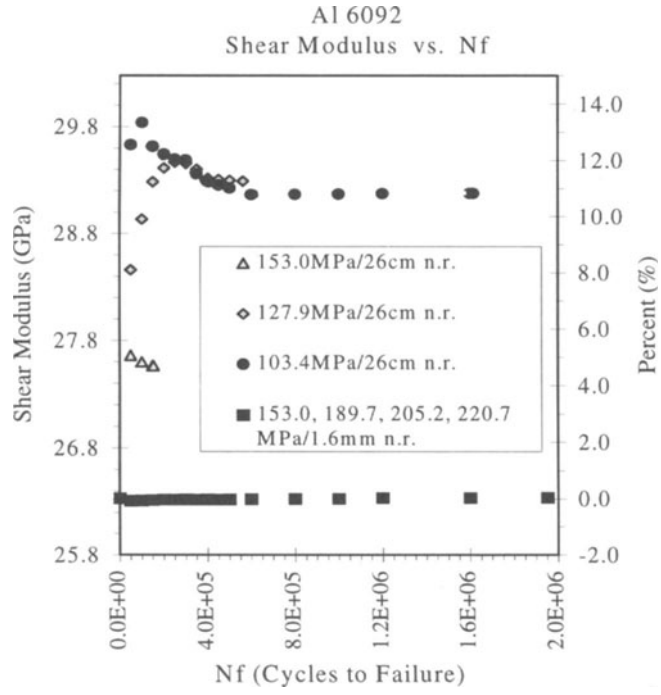

Figure 6. Shear Modulus-Cycles to Failure plot for monolithic Al 6092 specimens.

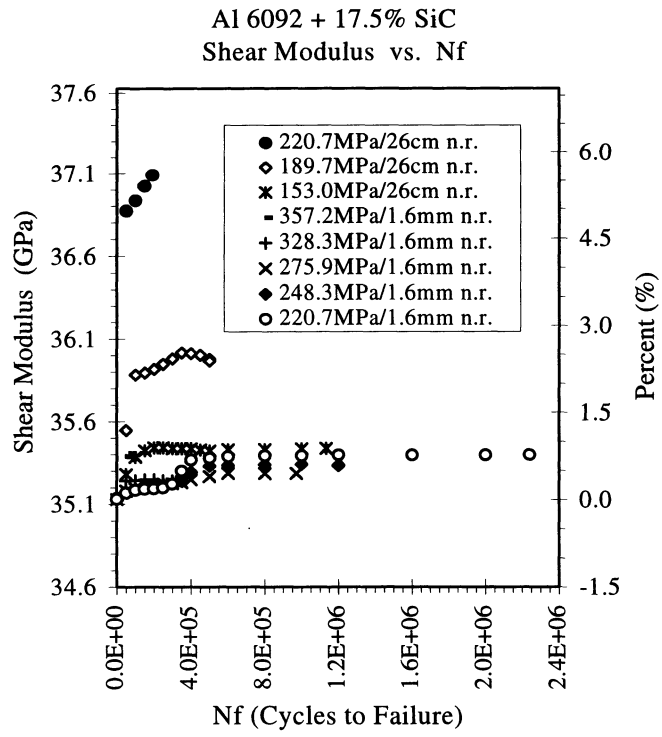

Figure 7. Shear Modulus- Cycles to Failure plot for Al 6092 + 17.5% SiC_p specimens.

Referring to Figure 7, the Shear Modulus-Cycles to Failure plot for the composite specimens shows a similar behavior to the longitudinal modulus behavior in Figure 5, in which both elastic moduli increase with increasing peak stress. It is further observed that for the composites, there is an increase in the shear modulus of up to about 5.5%. This value is higher compared to that in the monolithic aluminum, a ratio of 2 between the two being observed here. Since shear modulus is directly proportional to the square of the shear wave velocity v_s, it is indicative of the shear wave velocity in composites being more sensitive to fatigue than its longitudinal wave velocity.

It is observed that the elastic constants behavior for the monolithic aluminum is opposite to that of the composite i.e. the elastic constants increases with decreasing peak stress in the former (Figures 4 and 6) while in the latter, the elastic constants increases with increasing peak stress (Figures 5 and 7). In general, the elastic constants for both materials increase sharply with fatigue life especially in low cycle fatigue (LCF).

SUMMARY

At the same peak stress, the composite has a much longer fatigue life than that of the monolithic aluminum. At large notch in both monolithic and composite, ultrasonic velocities increase sharply with number of cycles at low cycle fatigue but remain unchanged or slightly decreased in the high cycle regime; changes in longitudinal, or shear modulus as a function of fatigue life are larger in monolithic aluminum than in composites, by a factor of 8-10 in longitudinal and a factor of 1.8-2 in shear. At large notch, changes in shear modulus as a function of fatigue life in composites are larger than

its longitudinal modulus. This indicates that shear velocity in composites is more sensitive to fatigue than longitudinal velocity. For all specimens at small notch, changes in longitudinal or shear velocity are much smaller than those specimens at large notch. Also, changes in ultrasonic velocities due to fatigue are much higher (more than 10) at large notch radius.

ACKNOWLEDGEMENT

This research is supported by the U.S. Army Research Office under contract no. DAAH04-95-1-0566. Mr. Nuñez would also like to acknowledge the support of the Dept. of Science and Technology and Western Institute of Technology (Philippines).

REFERENCES

1. Noguchi, M., *Adv. Mater. Processes* 143, No. 6, 20-26 (June 1993)
2. Dermarkar, S., *Metals and Mater.* 2, 144-147 (1986)
3. Mangin, C., Isaacs, J. and Clark, J., " MMCs for Automotive Engine Applications", *JOM* (Feb. 1996)
4. Srivatsan, T. and Soboyejo, W., *Eng. Frac. Mech.* 52, No. 3, 467-491 (1995)
5. Bergengren, Y., Larsson, M. and Melander, A., *Mat. Sci. and Tech.*, 11, 1275-80 (Dec. 1995)
6. Klar, E., Berry, D. and Samal, P., *Int. J. of Powder Metallurgy* 31, p.317 (Oct. 1995)
7. Mohrbacher, H., *"Temperature Dependence of Nonlinear Ultrasonic Effects"*, Master's Thesis, Univ. of Houston, Houston, TX (May 1991)
8. Lee, D., Salama, K and Schneider, E., *"Ultrasonic Characterization of SiC reinforced Aluminum"*, Proceedings of the 3rd Symp. on Nondestructive Characterization of Materials, Saarbrucken, FRG (Oct. 1988)
9. Agarwal,A., *Processing and Characterization of Aluminum/Silicon Carbide Composites Manufactured by Hot Isostatic Pressing* Master's Thesis, Univ. of Houston, Houston, TX (Aug. 1995)
10. Boving, K., Ed., "Non-destructive examination methods for condition monitoring" *NDE Handbook,* Teknisk Forlag A/S (Danish Technical Press) 1989
11. Frick, J., Ed., *Woldman's Engineering Alloys*, 8th ed., ASM Int'l., Mat'ls. Park, OH
12. Wahnschaffe, J., *The Evaluation of Fatigue Behavior in Metal-Matrix Composites using Ultrasonic Techniques,* Master's Thesis, University of Houston, Houston, TX (1994)
13. ASTM E 466 - 76: "Constant Amplitude Axial Fatigue Tests of Metallic Materials" *ASTM Standards*, Part 10, 631-636
14. Weixing, Y., Kaiquan, X. and Yi, G., *Int. J. Fatigue* 17, No. 4, 245-251 (1995)
15. Peterson, R., *Stress Concentration Factors* John Wiley & Sons, Inc. (1974)
16. Peterson, R., *Notch Sensitivity, Metal Fatigue*, (Sines, G. and Waisman, J., Ed.), McGraw-Hill, New York, 293-306 (1959)
17. Papadakis, E., *J. Acoust. Soc. Am.* 40, 1045-1051 (1967)
18. PANAMETRICS, INC. Journal/Catalog, *Ultrasonic Transducers for nondestructive testing*, NDT Division, Waltham MA (Apr. 1993)